



Cairo University

# **A BINDING SCHEME TO MINIMIZE THINNING OF FORMED TAILOR WELDED BLANKS**

By

**Mahmoud Samir Ahmed El-Sayed Seyam**

A Thesis Submitted to the  
Faculty of Engineering at Cairo University  
in Partial Fulfillment of the  
Requirements for the Degree of  
**MASTER OF SCIENCE**  
in  
**Mechanical Design and Production Engineering**

FACULTY OF ENGINEERING, CAIRO UNIVERSITY  
GIZA, EGYPT  
2018

**A BINDING SCHEME TO MINIMIZE THINNING OF  
FORMED TAILOR WELDED BLANKS**

By

**Mahmoud Samir Ahmed El-Sayed Seyam**

A Thesis Submitted to the  
Faculty of Engineering at Cairo University  
in Partial Fulfillment of the  
Requirements for the Degree of  
**MASTER OF SCIENCE**  
in  
**Mechanical Design and Production Engineering**

Under the Supervision of

**Prof. Dr. Abdalla S. Wifi**  
Department of Mechanical Design  
and Production Engineering  
Faculty of Engineering, Cairo  
University

**Assoc.Prof. Alaa El-Mokadem**  
Department of Mechanical Design  
and Production Engineering  
Faculty of Engineering, Cairo  
University

**Assoc.Prof. Mostafa Shazly**  
Mechanical Engineering Department  
Faculty of Engineering,  
The British University in Egypt

FACULTY OF ENGINEERING, CAIRO UNIVERSITY  
GIZA, EGYPT  
2018

Engineer's Name: Mahmoud Samir Ahmed El-Sayed Seyam  
Date of Birth: 14/11/1989  
Nationality: Egyptian  
E-mail: Mahmoud.s.seyam@cu.edu.eg  
Phone: +201094589646  
Address: 369/12 St/Alfardows Gardens/October City/Giza  
Registration Date: 1/10/2013  
Awarding Date: ..../..../2018  
Degree: Master of Science  
Department: Mechanical Design and Production Engineering



Supervisors:

**Prof. Dr. Abdalla S. Wifi**

**Assoc.Prof. Alaa El-Mokadem**

**Assoc.Prof. Mostafa Shazly**

(Faculty of Engineering, The British University in Egypt)

Examiners:

**Prof. Dr. Abdalla S. Wifi**

(Thesis main advisor)

**Prof. Dr. Mohammed M. Megahed**

(Internal examiner)

**Prof. Dr. Mahmoud Mohamed M. Nemat-Alla** (External examiner)

(Deen of the Faculty of Engineering, Kafr El-Sheikh University)

Title of Thesis:

A Binding Scheme To Minimize Thinning of Formed Tailor Welded Blanks

Key Words:

Tailor Welded Blanks; Die-Forming; Analytical modeling; Finite Element Simulation; Experimental Work;

Summary:

The present work suggests a new binding scheme to reduce the thinning and weld line movement of TWBs. This scheme combines weld line constraining via counter pins while applying a lower BHF on the weaker side as compared to the stronger side via segmented binders to achieve minimum thinning in the final product. Adopting this scheme, an analytical model was developed for the plane strain 2D draw bending and the 3D box deep drawing processes to determine the required BHF and counter pin force values. Laboratory and numerical experiments were conducted to examine the developed analytical model and compare the proposed controlling scheme with other schemes. The experimental results showed that the new scheme is physically applicable and capable of providing reasonably accurate force values that sufficiently eliminate the weld line movement and enhance formability (substantial reduction in thinning).

The present study showed the merits of implementing the proposed scheme in cases where large thickness and/or strength ratio of the sheets comprising the TWB exist. In such cases, conventional segmented binders along with weld line clamping technique without any variation in the applied BHF at each side cannot prevent.

## **Acknowledgments**

I would like to express my gratitude to my parents, my wife and the rest of my family, thank you all for your limitless support. A special gratitude also goes to my supervisors for the valuable guidance.

## **Dedication**

I dedicate this work to all interested and knowledge eager folks.

# Table of Contents

<b>ACKNOWLEDGMENTS</b> .....	<b>I</b>
<b>DEDICATION</b> .....	<b>II</b>
<b>TABLE OF CONTENTS</b> .....	<b>III</b>
<b>LIST OF TABLES</b> .....	<b>V</b>
<b>LIST OF FIGURES</b> .....	<b>VI</b>
<b>NOMENCLATURE</b> .....	<b>X</b>
<b>ABSTRACT</b> .....	<b>XI</b>
<b>CHAPTER 1 : INTRODUCTION</b> .....	<b>1</b>
1.1.HISTORICAL BACKGROUND .....	1
1.2.MOTIVATION AND THESIS ORGANIZATION .....	4
<b>CHAPTER 2 : TECHNICAL REVIEW</b> .....	<b>7</b>
2.1.TAILORED BLANKS: DEFINITION .....	7
2.2.TOOL DESIGNS FOR TAILOR WELDED BLANKS .....	7
2.3.FORMABILITY OF TAILOR WELDED BLANKS .....	9
2.4.WLM AND RELATION TO FORMABILITY ENHANCEMENT.....	10
2.5.MODELS FOR WLM CONTROL .....	13
<b>CHAPTER 3 :A NEW BINDING FORCE SCHEME:ANALYTICAL MODEL</b>	
<b>15</b>	
3.1.ASSUMPTIONS AND GOVERNING EQUATIONS .....	15
3.1.1.Force equations.....	15
3.1.2.Stress-Strain Equations.....	16
3.1.3.Elongation Equations.....	17
3.2.ANALYTICAL FORCE SCHEME MODEL FOR THE U-DRAW BENDING PROCESS.....	18
3.3.ANALYTICAL FORCE SCHEME MODEL FOR DEEP DRAWING OF BOX-SHAPED PARTS	
21	
<b>CHAPTER 4 : EXPERIMENTAL VERIFICATION OF THE NEW FORCE SCHEME</b> .....	<b>23</b>

4.1.U-SHAPE MODEL .....	23
4.2.BOX SHAPE MODEL.....	26
<b>CHAPTER 5 : FINITE ELEMENT MODELING AND VERIFICATION OF THE NEW FORCE SCHEME .....</b>	<b>33</b>
5.1.U-DRAW BENDING MODEL .....	33
5.1.1.Advantage of the new force scheme over other schemes (including material anisotropy in FE simulations).....	38
5.2.BOX-DRAWING PROCESS .....	42
<b>CHAPTER 6 RESULTS AND DISCUSSIONS .....</b>	<b>49</b>
6.1.NEW SCHEME VERIFICATION: SIMULATION RESULTS .....	49
6.1.1.Draw-Bending Model.....	49
1.1.1.1. Extreme case .....	57
6.1.2.Rectangular Box-Shaped Model.....	61
6.2.NEW SCHEME VERIFICATION: EXPERIMENTAL RESULTS .....	62
6.2.1.U-Draw Bending Model.....	62
6.2.2.Rectangular Box-Shaped Model.....	63
<b>CHAPTER 7 : CONCLUSIONS AND FUTURE WORK.....</b>	<b>67</b>
7.1.CONCLUTIONS .....	67
7.2.FUTURE WORK.....	67
<b>APPENDIX A: GEOMETRICAL MODEL.....</b>	<b>68</b>
<b>APPENDIX B: MATLAB CODE.....</b>	<b>70</b>
<b>APPENDIX C: PUBLISHED WORK .....</b>	<b>71</b>
<b>REFERENCES.....</b>	<b>89</b>

## List of Tables

Table 1: Characteristics of the TWB used in the U-Draw Bending experiments (According to ASTM-E8).....	25
Table 2: Characteristics of the TWB used in the Box deep Drawing experiments (According to ASTM-E8).....	31
Table 3: U-Draw Bending parameters for the FE model.....	34
Table 4: Comparison between the FE model and the experiment of case C .....	37
Table 5: Bench mark model parameters .....	40
Table 6: Input values for the selected case studies. ....	41
Table 7: Box model parameters .....	46
Table 8: Experimental and FE results for model verification.....	63

## List of figures

Figure 1.1: Ford Model-T Coupe, 1926[2] .....	1
Figure 1.2: Unitized Body, (a) Nash Ambassador 1942, (b) Fiat-1400 1950 [3] .....	2
Figure 1.3: Tailor Welded Blank (TWB) by Budd Company, patented 1964 [4] .....	2
Figure 1.4: Ultra-Light Steel Body, ULSAB report 2001[8] .....	3
Figure 1.5: Mass distribution of the ULSAB chassis based on the applied manufacturing technique[8] .....	3
Figure 1.6: Application of TWBs (red color)in Automobile chassis, ULSAB 1998[8] .....	4
Figure 1.7: The world’s first five-piece hot-stamped laser-welded door ring and b-pillar, Utility Vehicle of the Year, the Chrysler Pacifica 2017[10] .....	4
Figure 1.8: Selected processes for the current study. (a) Conventional U-Draw Bending Process, (b) Conventional Box-Deep Drawing Process .....	5
Figure 2.1: Schematic of a car door panel stamped from a Tailor Welded Blank.....	7
Figure 2.2: Thickness step direction, (Left) downward direction, (Right) Upward direction .....	8
Figure 2.3: Tool modifications for dissimilar thickness TWBs, (a) Stepped-Punch configuration (b) Stepped Die Configuration. ....	8
Figure 2.4: Movement of the boundary line between two adjacent dissimilar parent sheets (aka WLM).....	10
Figure 2.5: WLM elimination with Segmented-Binder Technique, $BHF_s < BHF_w$ .....	11
Figure 2.6: WLM elimination with Clamping-Pin technique.....	11
Figure 2.7: WLM elimination with Counter-Punch technique, Morishita 2012.....	12
Figure 2.8: Effect of Counter Punch on WLM of 0.6mm/1.16mm mild steel TWBs (a) no counter punch is used, (b) Half counter Punch applied only at the thicker side, (c) full counter punch applied as shown in Figure 2.7 [22] (Enhanced figures).....	12
Figure 3.1 Draw Bending of U-Shaped Part: Material flow pattern.....	16
Figure 3.2: Draw Bending of U-Shaped Part: Profile segmentation for each side.....	16
Figure 3.3: Blank holding configurations: Case 1; the flange is completely under binder with decreasing blank holding area.....	19
Figure 3.4: Case 2; the flange is partially constrained under a constant blank holding area.....	20

Figure 3.5: Biaxial condition at the bottom section – one side of the TWB is illustrated .....	22
Figure 4.1: Assembly and dimensions of the die set used in the experimental work. .	24
Figure 4.2: U-Draw Bending of a homogeneous blank, drawing height = 50mm .....	24
Figure 4.3: TWB sample, U draw bending experiments .....	25
Figure 4.4: Vickers Hardiness Test - HAZ width = 17mm .....	25
Figure 4.5: Assembly and dimensions of the die set used for Box Deep Drawing experimental work. ....	27
Figure 4.6: The final die configuration used in experiments (with modified counter pin) .....	28
Figure 4.7: Top view, (a)U-Draw Bending Die with segmented binder and counter pin .....	29
Figure 4.8: A sample of the drawing trials with different initial blank shapes.....	29
Figure 4.9: Final test trial, (a) optimum Blank geometry and BHF (dimensions in mm), (b) Produced rectangular box, drawing height =40mm .....	30
Figure 5.1: Configuration of the produced FEA model.....	34
Figure 5.2: Comparison between the kinetic energy (KE=N.mm) and internal energy (IE=N.mm) of the FE model, step time=0.01s, $KE < 7.5\% IE$ .....	35
Figure 5.3: Demonstration of the four different FE models, (a) WL properties included, 3600 elements, (b) weld line not included, 2700 elements, approximate element size= 1mm x 0.195mm (c) ) WL properties included, 15216 elements (d) weld line not included, 5700 elements.....	35
Figure 5.4: Comparison between the four models during the dynamic step time, thin flange displacement (upper line), weld line movement (middle line), thick flange displacement (lower line), and displacement in mm .....	36
Figure 5.5: Unloaded profile, overlay plot of the four models at the end of the static step .....	36
Figure 5.6: Comparison between the FE model and the experiment of case C, (a) FE model (Figure 5.3- b) , (b) Experiment.....	37
Figure 5.7: Comparison between the FE model and the experiment of case F, (a) FE model, (b) Experiment .....	37
Figure 5.8: Schematics for each of the compared WLM controlling schemes.....	39
Figure 5.9: Bench mark model parameters [28] .....	40

Figure 5.10: Simulation of the Benchmark Test, (Vertical displacement of the flange tip =18.15 mm), spring back angle (angle between the flange and the horizontal line = 0.22) .....	41
Figure 5.11: Draw-bending process for all cases with process and geometrical input parameters.....	41
Figure 5.12: Morishita experimental case (A+B ) [22].....	43
Figure 5.13: Half the Die Set (a) experimental work by Morishita et al. and (b) proposed approach.....	43
Figure 5.14: TWB mesh configuration, (a) 5065 linear quadrilateral elements of type S4R and 1516 linear triangular elements of type S3R with 5 thickness integration points), (b) 9985 linear quadrilateral elements of type S4R and 1516 linear triangular elements of type S3R with 9 thickness integration points).....	44
Figure 5.15: Path directions for thickness comparisons .....	44
Figure 5.16: Thickness distribution along 90° path, (a) Adopted mesh density Figure 5.14-a, (b) Doubled mesh density Figure 5.14-b.....	45
Figure 5.17: Comparison between the kinetic energy (KE=N.mm) and internal energy (IE=N.mm) of the FE model, step time=0.01s, KE < 4% IE.....	45
Figure 5.18: Thickness strain distribution for experimental work by Morishita et al. [22]and FE simulation along. a 0° path. b 45° path. c 90° path. The thick side is located on the positive x-axis .....	47
Figure 6.1: Forces predicted by the developed analytical model, (a) Blank holding force ratio (BHFw/BHFs), (b) Clamping Force (aka. Counter pin force (Fpin)) .....	50
Figure 6.2: Forces predicted by the developed analytical model in each case and used in the FE simulations. ....	51
Figure 6.3: Counter pin configuration. ....	52
Figure 6.4: Current flange length vs. punch position (new force scheme applied). ....	52
Figure 6.5: Final length ratio between the strong and weak sides. ....	53
Figure 6.6: Weld line movement relative to punch position, horizontal (HWLM). ....	53
Figure 6.7: BHF inputs for the segmented binders alone technique.....	54
Figure 6.8: Normalized overall thinning strain: (a) Weaker Side, (b) Stronger Side ..	56
Figure 6.9: Case 3, (a) Conventional Scheme , (b) Counter pin alone scheme, (c) Segmented binders alone scheme, (d) New force scheme .....	57
Figure 6.10: Extreme case – conventional scheme - Identical BHF=5000N - Punch position= 18mm .....	58

Figure 6.11: Thickness strain along the blank top surface at different punch depths – conventional scheme.....	58
Figure 6.12: Extreme case – counter pin alone scheme - Identical BHF=5000N - Punch position = 49mm .....	59
Figure 6.13: Thickness strain along the blank top surface at different punch depths – counter pin alone scheme.....	59
Figure 6.14: Extreme case – New force scheme - BHF <sub>s</sub> = 10000N, BHF <sub>w</sub> = 850N – end of the forming step- Punch position=75mm.....	60
Figure 6.15: Maximum absolute thickness strain at the weaker side at different punch positions. ....	60
Figure 6.16: Thickness strain distribution for FE model based Morishita et al. [4] approach and the new force scheme: (a) 0 degree path, (b) 45 degree path, and (c) 90 degree path. The thick side is located on the positive x-axis.....	62
Figure 6.17: Experimental comparisons between free weld line and new scheme: (a) Cases A and D, (b) Cases B and E, and (c) Cases C and F.....	63
Figure 6.18: Rectangular drawn box with no counter punch and equal BHF.....	64
Figure 6.19: Rectangular drawn box of 35mm height, (a) New scheme , (b) Counter pin alone scheme .....	64
Figure 6.20: Path directions for thickness comparisons, grid size =5mm .....	64
Figure 6.21: Thickness distribution for experimental work on rectangular box-shaped drawn parts: (a) 0 degree path, (b) 45 degree path, and (c) 90 degree path.....	66

## Nomenclature

$F$	Tensile force along the deformed profile (normal to the sheet thickness)
$BHF_s$	Blank holding force on the stronger side
$BHF_w$	Blank holding force on the weaker side
$F_{pin}$	Clamping force along the weld line
$\mu_p$	Friction coefficient at the weld line
$\mu_s$	Friction coefficient at the stronger side
$\mu_w$	Friction coefficient at the weaker side
$K$	Strength coefficient (in the maximum principal direction)
$n$	Strain hardening exponent
$L_o$	Original length (for each parent sheet s & w)
$t_o$	Original thickness (for each parent sheet s & w)
$L$	Current length (for each parent sheet s & w)
$t$	Current thickness (for each parent sheet s & w)
$\Delta L_{s_{tot}}$	Total increase in the original length (the total elongation) of the stronger parent sheet
$\Delta L_{w_{tot}}$	Total increase in the original length (the total elongation) of the weaker parent sheet
$c$	Die/Punch clearance
$R_d$	Die corner radius
$R_p$	Punch corner radius
$Y$	Punch current vertical position
$\Theta$	Wrap Angle
$M$	internal bending moments
$X_w$	Initial Weld Line Position
$\sigma$	Effective stress
$\epsilon$	Effective strain
$\alpha$	Stress ratio $\frac{\sigma_2}{\sigma_1}$
$\beta$	Strain ratio $\frac{\epsilon_2}{\epsilon_1}$

## Abstract

Die-Forming of Tailor Welded Blanks (TWBs) is currently used to produce body panels by the majority of automotive manufacturers. The high material utilization and structural rigidity combined with weight reduction and controlled crash behavior are some of many reasons behind the fast spread of this non-traditional technique. Processing of TWBs has been subjected to intensive research over the past four decades. Still, the field is frequently updated with new ideas and innovations for better utilization of such inherently inhomogeneous Blanks.

This work presents a new force scheme to minimize thinning and Weld Line Movement (WLM) during TWBs die forming. The scheme is applied by means of weld line counter-pins and blank holding segmented binders. An analytical model is developed to provide the required set of forces (Binders and counter pins forces) depending on the TWB properties and die geometry. The model is developed for the U-Draw Bending and Rectangular Box-Shaped Deep Drawing processes following the Marciniak's 2D and 3D stamping approaches. Given the blank geometry/material properties, tool geometry, and the input Blank holder force (binder force) at one of the parent sheets, the model provides the remaining binder forces and the minimum required counter pin force. Depending on the strength of each parent sheet, the estimated forces produce identical elongations in each parent sheet normal to the weld line direction in order to prevent the WLM.

Two different die sets were custom-manufactured for the application of segmented binders and counter-pins. The Die sets were used to verify the new force scheme by applying the predicted forces from the analytical model as inputs in a series of U-Draw Bending and Box-Deep Drawing laboratory experiments. Additional experiments and finite element simulations were used to present the advantage of the new force scheme over other existing schemes.

The experimental results demonstrate the practical feasibility of the new force scheme and validate its capability to minimize thinning as well as WLM. The laboratory experiments and Finite Elements (FE) simulations based on the proposed force scheme also show significant improvement in formability when compared to separate use of either weld line clamping pins or the segmented binders, and show that it can prevent eminent potential failure of the drawn part.

# Chapter 1 : Introduction

## 1.1. Historical Background

By the end of the First World War, steel sheets were gradually replacing wood in the production of vehicles external bodies. Back then, all automobiles were manufactured based on a concept known as body-on-frame (BOF). A powertrain was assembled by chassis manufacturers on a rigid frame as an independent drivable unit while the remaining of the vehicle, the upper body, was separately made by coachbuilders in internal body shops. The two units were later assembled to produce a finished car like the Ford T-Coupe in Figure 1.1. The BOF concept is still adopted by some SUVs and pickup trucks manufacturers but rarely seen in smaller passenger cars at the present time [1][2].

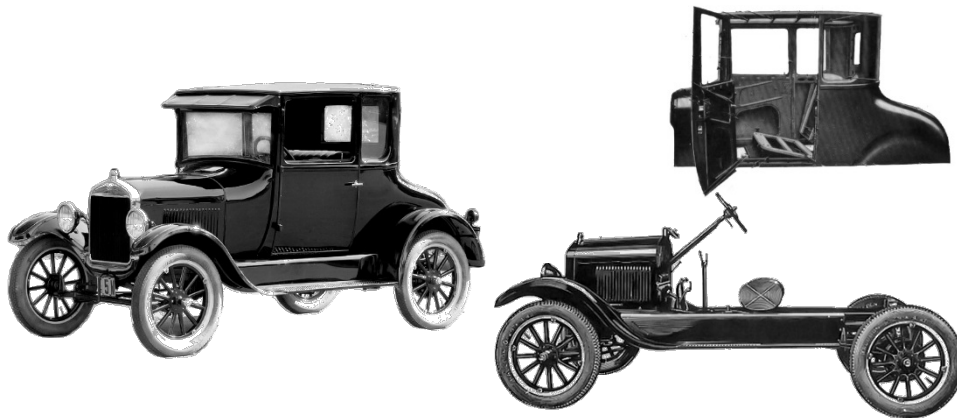


**Figure 1.1: Ford Model-T Coupe, 1926[2]**

In developed countries, the increasing demand for higher top speeds and less power consumption during the interwar era (between both World Wars) was forcing the automotive industry toward light-weight bodies with higher structural integrity. After the Second World War, vehicles designs started to shift from BOF concept to the unitized body concept. In which, the upper body and chassis were replaced by a single integral skeleton covered by various die-formed steel panels (aka monocoque chassis) as shown in Figure 1.2. The technology was developed early in the 1920s by European manufacturers in collaboration with the USA Budd Company. However, it wasn't until the late 1950s for the technology to be widely used in association with certain advances in sheet metal welding technology. Soon after, unitized body designs became standard for most commercial passenger-cars [1][3].